Geosci. Model Dev. Discuss., 7, 1649–1669, 2014
www.geosci-model-dev-discuss.net/7/1649/2014/
doi:10.5194/gmdd-7-1649-2014
© Author(s) 2014. CC Attribution 3.0 License.

Geoscientific Model Development Discussions
Open Access

This discussion paper is/has been under review for the journal Geoscientific Model Development (GMD). Please refer to the corresponding final paper in GMD if available.

Development of a semi-parametric PAR partitioning model for the contiguous US

J. C. Kathilankal[1], T. L. O'Halloran[2], A. Schmidt[3], C. V. Hanson[3], and B. E. Law[3]

[1]LI-COR Inc. 4647 Superior Street, Lincoln, NE, 68504, USA
[2]Sweet Briar College, Department of Environmental Science, Sweet Briar, VA, 24595, USA
[3]Department of Forest Ecosystems and Society, College of Forestry, Oregon State University, 321 Richardson Hall, Corvallis, OR 97331, USA

Received: 22 January 2014 – Accepted: 14 February 2014 – Published: 6 March 2014

Correspondence to: J. C. Kathilankal (james.kathilankal@licor.com)

Published by Copernicus Publications on behalf of the European Geosciences Union.

Abstract

A semi-parametric PAR diffuse radiation model was developed using commonly measured climatic variables from 44 site-years of data from 9 AmeriFlux sites. The model has a logistic form and improves upon previous efforts, using a larger data set and physically viable climate variables as predictors, including relative humidity, clearness index, surface albedo, and solar elevation angle. Model performance was evaluated by comparison with a simple cubic polynomial model developed for the PAR spectral range. The logistic model outperformed the polynomial model with an improved coefficient of determination and slope relative to measured data (logistic: $R^2 = 0.85$; slope = 0.86; cubic: $R^2 = 0.82$; slope = 0.83), making this the most robust PAR-partitioning model for the US subcontinent currently available.

1 Introduction

Photosynthetically active radiation (PAR) is the 0.4–0.7 µm spectral range that is absorbed by plants and drives the process of photosynthesis (McCree, 1972). PAR at the ground surface has two primary incoming streams, diffuse and direct; which are significantly affected by the amount of clouds and aerosols in the atmosphere. These two radiant components differ in the way they transfer energy through plant canopies thus affecting canopy photosynthesis processes differently than what would occur at the leaf scale (Misson et al., 2005). Increased diffuse PAR fraction (the ratio of diffuse or isotropic PAR to total PAR (diffuse + direct beam)) in the atmosphere has been correlated with higher light use efficiency and increased CO_2 assimilation (e.g. Weiss and Norman, 1985; Gu et al., 1999, 2002, 2003; Knohl et al., 2008; Mercardo et al., 2009; Still et al., 2009). Many of these studies utilize models of diffuse radiation (usually in the 0.15 to 4.0 µm shortwave range) to estimate the diffuse fraction rather than direct measurements.

GMDD
7, 1649–1669, 2014

CC BY

Diffuse PAR can be estimated from models that range in complexity from spectral parameterization schemes like SPCTRAL2 (Bird and Riodan, 1986) and SMARTS2 (Gueymard, 1995) to simple linear regression models relating diffuse radiation fraction to extra terrestrial PAR (Hassika and Berbigier, 1998; Tsubo and Walker, 2005). Jacovides et al. (2009) developed a third order polynomial model after applying 25 point moving average on clearness index (k_{tp}) (the ratio of global irradiance to extraterrestrial irradiance) data collected over a three year period over Athens, Greece. Butt et al. (2010) used a proxy cloud fraction (ratio of calculated total solar irradiance at a surface to the measured) to estimate diffuse PAR fraction.

Most diffuse fraction models are developed for global solar irradiation and very few models are developed from PAR data sets. The models developed for global solar radiation have been used in studies to convert the diffuse global solar irradiance to diffuse PAR fractions (e.g. Gu et al., 2002). Regression type models of diffuse shortwave radiation usually employ linear (e.g. Orgil and Hollands, 1977; Reindl et al., 1990), logistic (Boland et al., 2001; Ridley, 2010) or higher order polynomial type (e.g. Erbs et al., 1982; Spitters et al., 1986; Chandrasekaran and Kumar, 1994; Miguel et al., 2001; Oliveria et al., 2002; Jacovides et al., 2006) equations relating clearness index (k_{tp}) to estimate diffuse fraction (k_{dp}). Reindl et al. (1990) used multiple regression analysis and identified air temperature, dew point and sine of the solar elevation angle as important parameters determining the partitioning of total irradiance into diffuse and direct components. Solar elevation angle and clearness index were used as inputs in models developed by Maxwell (1987) and Skartveit and Olseth (1987). Other parameters used in modeling diffuse fraction include dew point temperature, albedo and hourly variability index (root mean square difference between clearness index of an hour in question with respect to its preceding and succeeding hour) e.g. Perez et al. (1992) and Skartveit et al. (1998). The BRL model (Ridley et al., 2010) uses hourly clearness index, apparent solar time, solar elevation angle, daily clearness index and a persistence index similar to the variability index to calculate the diffuse fraction. Muneer and

GMDD
7, 1649–1669, 2014

cc BY

Munawwar (2006) used sunshine fraction, cloud fraction and air mass along with clearness index in predicting the diffuse fraction of global irradiance.

The objective of our study is to develop a simple semi-parametric diffuse PAR model applicable for the US subcontinent, employing the AmeriFlux (Hargrove et al., 2003) data set of above-canopy observations that have high spatio-temporal resolution. Development of such a model will aid future investigations of the effect of diffuse radiation on photosynthesis and light-use efficiency in response to climate. Although diffuse radiation is not regularly measured at all AmeriFlux sites, multiple year records from 9 sites are available for model development. The model presented here is developed with a dataset that is larger and more temporally and spatially diverse than any previous efforts, making it the most robust and broadly applicable diffuse PAR model developed to date.

2 Methodology and data analysis

The dataset used for model development and testing consists of multiple year records of PAR and diffuse fraction obtained from the AmeriFlux network. A detailed description of the sites utilized in this study is presented in Table 1. The sites selected consist of forested ecosystems and croplands covering a wide latitude range (35–46° N). The diffuse fraction data are mostly obtained using the BF3 sensor (Delta-T devices, Cambridge, UK). The BF3 sensor uses an array of photodiodes with a shading pattern that provides shade to some of the photodiodes while others remain exposed. This instrument has a resolution of 1 $\mu mol\, m^{-2}\, s^{-1}$ and an accuracy of 15 %. The data from BF3 sunshine recorders have been used in other studies relating cloud fraction to diffuse fraction (Butt et al., 2001).

For our study, data collected when solar elevation angles were < 10° were removed to avoid cosine response issues. Although the data set contained records in hourly and half hourly formats, we averaged data to obtain hourly values for consistency and removed outliers. The hourly radiation values were checked against the

GMDD
7, 1649–1669, 2014

quality controls proposed by the European Commission Daylight. This quality control eliminates data points based on the following criteria: Rd > 1.1; RS, RS > 1.2RE; Rd > 0.8RE; RS< 5 W m^{-2} and Rb >RE, where Rd is the total diffuse radiation Rs is the total incoming solar irradiance, RE is the extra terrestrial irradiance and Rb is the direct normal irradiance.

Data points were eliminated when hourly rainfall values were greater than 5 mm, relative humidity values were 100 %, or when dew point exceeded air temperature, as under these conditions, the measurement accuracy might be affected by water droplets formed on the sensor. After implementing the quality control check, the dataset consisted of 106 670 hourly records from 44 site years.

Extraterrestrial PAR was calculated with solar elevation angle at a location according to

$$R_E = R_C[1 + 0.033\cos(360t_d/365)\sin\beta] \tag{1}$$

where, R_C is the solar constant (2776.4 µmol m^{-2} s^{-1}, Spitters et al., 1986); sin β is the sine of the solar elevation angle and t_d is the day number since 1 January.

3 Model development

The model developed here is similar in structure to the multi-predictor logistic model (BRL) developed by Ridley et al. (2010) for global solar irradiance, except we use additional predictors that directly affect the diffuse fraction and we also use a considerably larger data set. The predictors in the BRL model include daily clearness index (k_t), sine of the solar elevation angle (αS), persistence index (ψ) and apparent solar time (AST).

$$k_d = \frac{1}{1 + \exp(-5.38 + 6.63k_t + 0.006\,\mathrm{AST} - 0.007\beta + 1.75k_t + 1.31\psi)} \tag{2}$$

The logistical form of the model has been identified as more robust than previously published piecewise linear or other non-linear forms (Boland et al., 2001, 2008). The goal of our work is to develop a model that is constrained by more commonly measured micrometeorological variables, rather than estimated variables like persistence index. The important factors considered in this study are PAR clearness index (k_{tp}), relative humidity (RH), albedo (α) and sine of solar elevation angle (β). Clearness index is widely used in one predictor models for PAR partitioning (Jacovides et al., 2009) as it is directly related to cloud fraction. Relative humidity is positively related with cloud cover (Walcek, 1994) and a greater diffuse fraction is often associated with higher humidity values. The effect of relative humidity on the relationship between k_{tp} and k_{dp} is presented in Fig. 1a. Increased surface albedo resulting from changes in canopy reflectance or presence of snow can alter the diffuse fraction estimates. Skartveit et al. (1998) proposed a correction for clearness index estimation to account for the multiple reflections occurring between the surface and instrument dome when albedo is over 0.15. However in this study we consider albedo as a contributing factor to diffuse fraction as multiple reflections between the surface and clouds can enhance the diffuse fraction available for photosynthesis (Campbell and Norman, 2008; Knohl and Baldocchi, 2008; and Winton, 2005). Albedo of most vegetated surfaces can reach up to 0.25 and can vary widely as a function of leaf area index, disturbance history and snow cover. The effect of surface albedo on the relationship between k_{tp} and k_{dp} is presented in Fig. 1b. Increased albedo can result in increased diffuse fraction for the same clearness index compared to lower albedo values. The PAR diffuse fraction model developed in this study takes the logistic form

$$k_{dp} = \frac{1}{1 + e^{-z}},$$

where z is given as

$$z = a + bk_{tp} + c\mathrm{RH} + d\alpha + e\sin(\beta) \tag{3}$$

and a, b, c, d and e are fitted empirical coefficients determined in our analysis. The empirical coefficients were obtained by fitting the model to a randomly-selected two-thirds

cc BY

of the data set. The relationship presented in Eq. (3) tends to underestimate diffuse fraction under clear sky conditions (Fig. 2a). As a correction, a second logistic fit is applied to the data for $k_{tp} > 0.78$. The values of the coefficients for the logistic model along with their 95 % confidence intervals are presented in Table 2. The model performance is compared with a one predictor model developed by Jacovides et al. (2009). This model was selected for comparison as it was developed using data in the PAR spectral range and used a simple predictor (k_{tp}) that could be estimated for a large data set from multiple locations. This cubic polynomial model which relates diffuse PAR fraction as a function of smoothed PAR clearness index (moving average window size of 25) takes the following form after fitting to this data set:

$$k_{dp} = 0.747 + 2.486k_{tp} - 7.859k_{tp}^2 + 4.830k_{tp}^3 \quad (4)$$

The original cubic polynomial model had prescribed limits within which the model operated and constant values were assigned to k_{dp} values for k_{tp} values above and below a particular range. The modified cubic polynomial model presented in Eq. (4) is valid for $0.19 < k_{tp} < 0.89$, whereas for $k_{tp} \leq 0.19$, $k_{dp} = 0.966$ and $k_{tp} \geq 0.89$, $k_{dp} = 0.142$. These set points were chosen to provide a smooth transition from the inflection points in the model output. The model coefficients were estimated using a robust nonlinear regression method in MATLAB (Mathworks, Inc). The fit of data to the adjusted logistic model and the cubic model for the selected data set is presented in Fig. 2b and Fig. 2c. The percentage differences between measured diffuse fraction k_{dp} and modeled diffuse fraction k_{dpm} is plotted in Fig. 3 as a function of each of the predictor variables in unequally spaced bins with an equal number of data points.

The model fits were assessed by applying the remaining third of the data set that was not used in model development (evaluation data set) for statistical analysis. The comparison between measured and modeled diffuse PAR for the logistic and cubical model for the evaluation data set is provided in Fig. 4.

The performance of both models was further compared by using a bootstrap regression between the measured and modeled diffuse fractions with a data re-sampling of

GMDD
7, 1649–1669, 2014

CC BY

10 000 times to account for the errors in measuring the independent variable (measured diffuse fraction) from the evaluation data set. The results of the bootstrap regression comparison for the two models are presented in Table 3. The root mean square error percentage (RMSE %) (Jacovides, 2006) of the model fits to the evaluation data set is also presented in Table 3. The influence of seasonality on the logistic model accuracy was examined by plotting the RMSE (%) and R^2 of the regression between measured and modeled values as a function of the various months (Fig. 5) for the entire data set.

4 Discussion

The multi-parameter logistic model predicts different diffuse fractions for the same clearness index for different combinations of albedo, solar elevation angle and relative humidity. The percentage difference between measured and modeled diffuse fraction generally indicate an underestimation by the model. The largest differences are associated with clearness index values around 0.7, albedo values of 0.13, moderate relative humidity (between 40–50 %) and high solar elevation angles ($> 65^{\circ}$) (Fig. 3). The logistic model thus produces the largest errors under clear sky conditions, during the late morning and afternoon periods and when the atmosphere is dry. The cubic polynomial model evaluated in this study produces the largest errors during periods of high solar elevation angle, similar to the logistic model but in contrast to the original model, which exhibited maximum error during the early morning/late evening hours (Jacovides et al., 2010). The regression analysis indicates better performance of the logistic model over the cubic model, with a higher slope, lower intercept, and a larger coefficient of determination (R^2) (Table 3 and Fig. 4). The RMSE (%) values also indicate a comparatively lower error for the logistic model (23.16 %) compared to the cubic polynomial model (25.46 %). The errors in the developed model could be attributed to other confounding factors such as seasonal effects, changes in atmospheric turbidity caused by air pollution or aerosol loading, and location differences. The fact that

GMDD
7, 1649–1669, 2014

CC BY

a combined data set from different locations was used in this study can lead to minimization of the dependence of the k_{dp}–k_{tp} correlation on local conditions (Jacovides et al., 2006). The model performance stays constant throughout the year except for the period from September to December when the RMSE (%) decrease and the R^2 value increases. The largest RMSE (%) values were observed during the summer months, as in Jacovides et al. (2006) (Fig. 5).

5 Concluding remarks

A logistic diffuse radiation model was developed using a large hourly radiation dataset obtained from the AmeriFlux network. The model performance was evaluated against a cubic polynomial model and its strengths and weaknesses were assessed. The goal was to develop a diffuse PAR model that employs commonly measured climatic/weather variables as predictors and is applicable for sites in the contiguous US. The logistic model improves upon other PAR diffuse fraction models as it was developed using a large data set comprising of multi-year records from multiple sites. Future work includes application of this model to estimate diffuse radiation effects and contributions to annual net ecosystem exchange over various biomes represented by the AmeriFlux data.

Code availability

The model is a very simple logistic model and it can be implemented very easily in any programming software or spread sheet based software like MS excel. A Matlab based function is provided. This function requires inputs of incoming PAR, relative humidity, albedo and sine of the solar elevation angle.

GMDD
7, 1649–1669, 2014

CC BY

Supplementary material related to this article is available online at http://www.geosci-model-dev-discuss.net/7/1649/2014/ gmdd-7-1649-2014-supplement.zip.

Acknowledgements. This research was supported by the Office of Science (BER), US Department of Energy (DOE, Grant nos. DE-FG02-06ER64307 and DE-FG02-06ER64316). The authors also would like to thank the AmeriFlux Network for providing the data and making it publically available. We would like to thank the principal investigators of the participating sites and other technical staff who put together this data set and the AmeriFlux QA/QC laboratory at Oregon State University for helping to ensure the quality of data of the AmeriFlux database.

References

Baldocchi, D., Falge, E., Gu, L. H., Olson, R., Hollinger, D., Running, S., Anthoni, P., Bernhofer, C., Davis, K., Evans, R., Fuentes, J., Goldstein, A., Katul, G., Law, B., Lee, X. H., Malhi, Y., Meyers, T., Munger, W., Oechel, W., Paw U, K. T., Pilegaard, K., Schmid, H. P., Valentini, R., Verma, S., Vesala, T., Wilson, K., and Wofsy, S.: FLUXNET: a new tool to study the temporal and spatial variability of ecosystem-scale carbon dioxide, water vapor, and energy flux densities, B. Am. Meteorol. Soc., 82, 2415–2434, 2001.

Bird, R. E. and Riordan, C.: Simple solar spectral model for direct and diffuse irradiance on horizontal and tilted planes at the earth's surface for cloudless atmospheres., J. Clim. Appl. Meteorol., 25, 87–97, 1986.

Boland, J., Scott, L., and Luther, M.: Modelling the diffuse fraction of global solar radiation on a horizontal surface, Environmetrics, 12, 103–116, 2001.

Boland, J., Ridley, B., and Brown, B.: Models of diffuse solar radiation, Renew. Energ., 33, 575–584, doi:10.1016/j.renene.2007.04.012, 2008.

Butt, N., New, M., Malhi, Y., da Costa, A. C. L., Oliveira, P., and Silva-Espejo, J. E.: Diffuse radiation and cloud fraction relationships in two contrasting Amazonian rainforest sites, Agr. Forest Meteorol., 150, 361–368, 2010.

Campbell, G. S. and Norman, J. M.: An Introduction to Environmental Biophysics, Springer-Verlag, New York, 1998.
Chandrasekaran, J. and Kumar, S.: Hourly diffuse fraction correlation at a tropical location, Sol. Energy, 53, 505–510, 1994.
De Miguel, A., Bilbao, J., Aguiar, R., Kambezidis, H., and Negro, E.: Diffuse solar irradiation model evaluation in the North Mediterranean belt area, Sol. Energy, 70, 143–153, 2001.
Gu, L. H., Fuentes, J. D., Shugart, H. H., Staebler, R. M., and Black, T. A.: Responses of net ecosystem exchanges of carbon dioxide to changes in cloudiness: results from two North American deciduous forests, J. Geophys. Res.-Atmos., 104, 31421–31434, 1999.
Gu, L., Baldocchi, D., Verma, S. B., Black, T. A., Vesala, T., Falge, E. M., and Dowty, P. R.: Advantages of diffuse radiation for terrestrial ecosystem productivity, J. Geophys. Res., 107, 4050, doi:10.1029/2001JD001242, 2002.
Gu, L. H., Baldocchi, D. D., Wofsy, S. C., Munger, J. W., Michalsky, J. J., Urbanski, S. P., and Boden, T. A.: Response of a deciduous forest to the Mount Pinatubo eruption: enhanced photosynthesis, Science, 299, 2035–2038, 2003.
Gueymard, C. A.: Parameterized transmittance model for direct beam and circumsolar spectral irradiance, Sol. Energy, 71, 325–346, 2001.
Hargrove, W., Hoffman, F., and Law, B.: New analysis reveals representativeness of the AmeriFlux network, EOS T. Am. Geophys. Un., 84, 529, doi:10.1029/2003EO480001, 2003, 2003.
Hassika, P. and Berbigier, P.: Annual cycle of photosynthetically active radiation in maritime pine forest, Agr. Forest Meteorol., 90, 157–171, 1998.
Jacovides, C. P., Tymvios, F. S., Assimakopoulos, V. D., and Kaltsounides, N. A.: Comparative study of various correlations in estimating hourly diffuse fraction of global solar radiation, Ren. Energ., 31, 2492–2504, doi:10.1016/j.renene.2005.11.009, 2006.
Jacovides, C. P., Boland, J., Asimakopoulos, D. N., and Kaltsounides, N. A.: Comparing diffuse radiation models with one predictor for partitioning incident PAR radiation into its diffuse component in the eastern Mediterranean basin, Renew. Energ., 35, 1820–1827, 2009.
Knohl, A. and Baldocchi, D. D.: Effects of diffuse radiation on canopy gas exchange processes in a forest ecosystem, J. Geophys. Res.-Biogeo., 113, G02023, doi:10.1029/2007jg000663, 2008a.
Knohl, A. and Baldocchi, D. D.: Effects of diffuse radiation on canopy gas exchange processes in a forest ecosystem, J. Geophys. Res., 113, G02023, doi:10.1029/2007JG000663, 2008b.

CC BY

Mercado, L. M., Bellouin, N., Sitch, S., Boucher, O., Huntingford, C., Wild, M., and Cox, P. M.: Impact of changes in diffuse radiation on the global land carbon sink, Nature, 458, 1014-U1087, doi:10.1038/Nature07949, 2009.
Muneer, T. and Munawwar, S.: Improved accuracy models for hourly diffuse solar radiation, J. Sol. Energ. T. ASME, 128, 104–117, doi:10.1115/1.2148972, 2006.
Oliveira, A. P., Escobedo, J. F., Machado, A. J., and Soares, J.: Correlation models of diffuse solar-radiation applied to the city of Sao Paulo, Brazil, Appl. Energ., 71, 59–73, 2002.
Orgill, J. F. and Hollands, K. G. T.: Correlation equation for hourly diffuse radiation on a horizontal surface, Sol. Energy, 19, 357–359, 1977.
Perez, R., Ineichen, P., Seals, R., and Zelenkal, A.: Dynamic global to direct irradiance conversion models, ASHRAE Transations, 98, 354–369, 1992.
Reindl, D. T., Beckman, W. A., and Duffie, J. A.: Diffuse fraction correlation, Sol. Energy, 45, 1–7, 1990.
Ridley, B., Boland, J., and Lauret, P.: Modelling of diffuse solar fraction with multiple predictors, Renew. Energ., 35, 478–483, doi:10.1016/j.renene.2009.07.018, 2010.
Skartveit, A. and Olseth, J. A.: A model for the diffuse fraction of hourly global radiation, Sol. Energy, 38, 271–274, 1987.
Skartveit, A., Olseth, J. A., and Tuft, M. E.: An hourly diffuse fraction model with correction for variability and surface albedo, Sol. Energy, 63, 173–183, 1998.
Spitters, C. J. T., Toussaint, H., and Goudriaan, J.: Seperating the diffuse and direct component of global radiation and its implications for modeling canopy photosynthesis. 1. Component of incoming radiation, Agr. Forest Meteorol., 38, 217–229, 1986.
Still, C. J., Riley, W. J., Biraud, S. C., Noone, D. C., Buenning, N. H., Randerson, J. T., Torn, M. S., Welker, J., White, J. W. C., Vachon, R., Farquhar, G. D., and Berry, J. A.: Influence of clouds and diffuse radiation on ecosystem–atmosphere CO_2 and $(COO){-}O^{18}$ exchanges, J. Geophys. Res.-Biogeo., 114, G01018, doi:10.1029/2007jg000675, 2009a.
Still, C. J., Riley, W. J., Biraud, S. C., Noone, D. C., Buenning, N. H., Randerson, J. T., Torn, M. S., Welker, J., White, J. W. C., Vachon, R., Farquhar, G. D., and Berry, J. A.: Influence of clouds and diffuse radiation on ecosystem–atmosphere CO_2 and $CO^{18}O$ exchanges, J. Geophys. Res., 114, G01018, doi:10.1029/2007JG000675, 2009b.
Tsubo, M. and Walker, S.: Relationships between photosynthetically active radiation and clearness index at Bloemfontein, South Africa, Theor. Appl. Climatol., 80, 17–25, doi:10.1007/s00704-004-0080-5, 2005.

GMDD
7, 1649–1669, 2014

Development of a semi-parametric PAR partitioning model

J. C. Kathilankal et al.

CC BY

Walcek, C. J.: Cloud Cover and Its Relationship to Relative Humidity during a Springtime Midlatitude Cyclone, Mon. Weather Rev., 122, 1021–1035, doi:10.1175/1520-0493(1994)122<1021:CCAIRT>2.0.CO;2, 1994.

Winton, M.: Simple optical models for diagnosing surface–atmosphere shortwave interactions, J. Climate, 18, 3796–3805, 2005.

GMDD

7, 1649–1669, 2014

GMDD
7, 1649–1669, 2014

Development of a semi-parametric PAR partitioning model

J. C. Kathilankal et al.

Table 1. Site location and ecosystem type information.

Sl. No	Site Name	Location	Ecosystem type	Sensor
1	Bartlett Experimental Forest (US-Bar)	44.0646, 71.2881	Deciduous broadleaf forest	BF3
2	Flagstaff Managed Forest (US-FmF)	35.1426, 111.7273	Evergreen needleleaf forest	BF3
3	Flagstaff Unmanaged Forest (US-Fuf)	35.0890, 111.7620	Evergreen needleleaf forest	BF3
4	Flagstaff Wildfire (US-Fwf)	35.4454, 111.7718	Woody savannas	BF3
5	Mead Irrigated (US-Ne1)	41.16506, 96.4766	Croplands	BF3
6	Mead Irrigated Rotation (US-Ne2)	41.16487, 96.4701	Croplands	BF3
7	Mead Rain fed (US-Ne3)	41.17967, 96.4396	Croplands	BF3
8	Morgan Monroe State Forest (US-MMS)	39.3231, 86.4131	Deciduous broadleaf	BF3
9	University of Michigan Biological Station (US-UMB)	45.5598, 84.7138	Deciduous broadleaf	BF3

CC BY

Table 2. Logistic model coefficients for clearness index classes. The value given in the brackets is 95 % confidence interval.

Coefficients	$k_{tp}(\leq 0.78)$	$k_{tp} > 0.78$
a	3.452 (3.3424, 3.480)	−0.263 (−0.421, −0.105)
b	−7.508 (−7.546, −7.470)	−1.645 (−1.824, −1.467)
c	0.629 (0.607, 0.650)	0.861 (0.815, 0.907)
d	1.440 (1.405, 1.476)	0.597 (0.553, 0.639)
e	0.496 (0.476, 0.515)	−0.660 (−0.707, −0.614)

GMDD
7, 1649–1669, 2014

CC BY

Table 3. Model performance comparison using regression analysis. The values given in the brackets are the standard error of the estimtes obtained by resampling evaluaton data 10 000 times. The root mean square error (RMSE) estiamte from the measured and modeled values is also presented.

Model	Logistic model	Cubic model
slope	0.86 ($\pm 1.6 \times 10^{-5}$)	0.83 ($\pm 1.8 \times 10^{-5}$)
intercept	6.32×10^{-2} ($\pm 8.0 \times 10^{-6}$)	7.95×10^{-2} ($\pm 8.0 \times 10^{-6}$)
R^2	0.85 ($\pm 1.60 \times 10^{-5}$)	0.82 ($\pm 1.9 \times 10^{-5}$)
rmse (%)	23.16	25.46

GMDD
7, 1649–1669, 2014

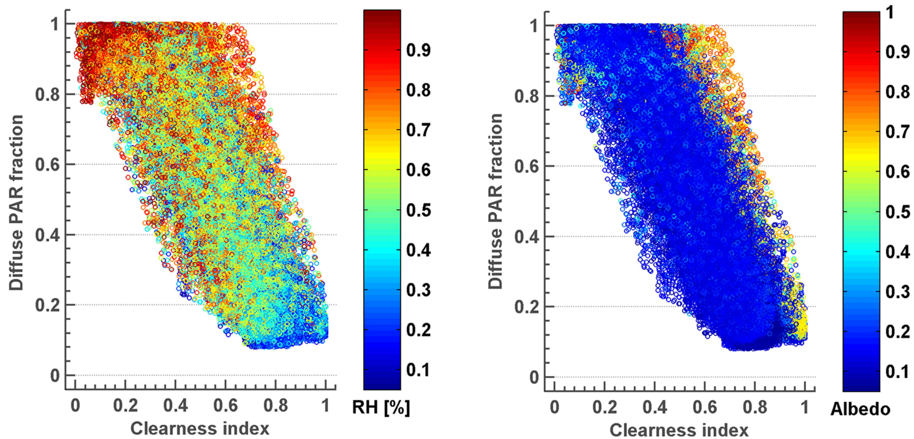

Fig. 1. Relative humidity and albedo effects of k_{tp}–k_{dp} relationship.

GMDD
7, 1649–1669, 2014

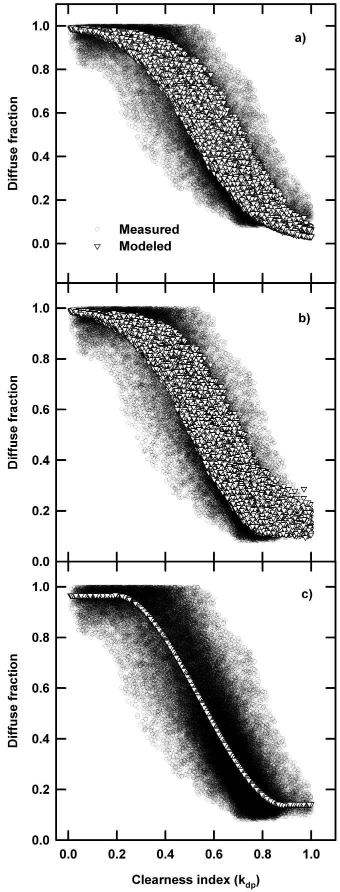

Fig. 2. Model fit for the proposed multi-parameter logistic model (**a** and **b**) and cubic model **(c)**.

CC BY

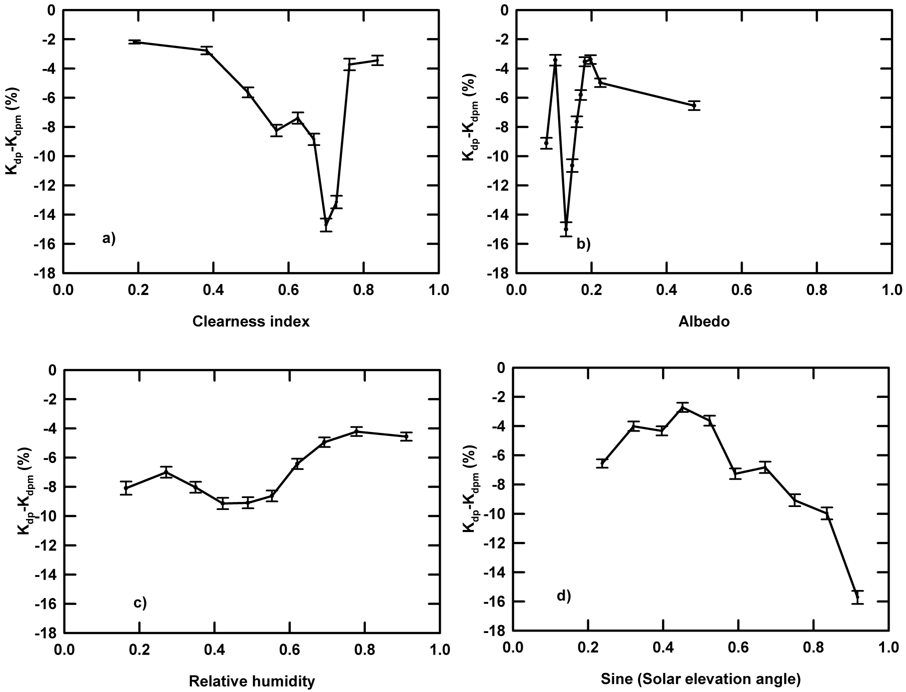

Fig. 3. Percentage differences between measured and modeled diffuse radiation as a function of predictor variables.

GMDD
7, 1649–1669, 2014

CC BY

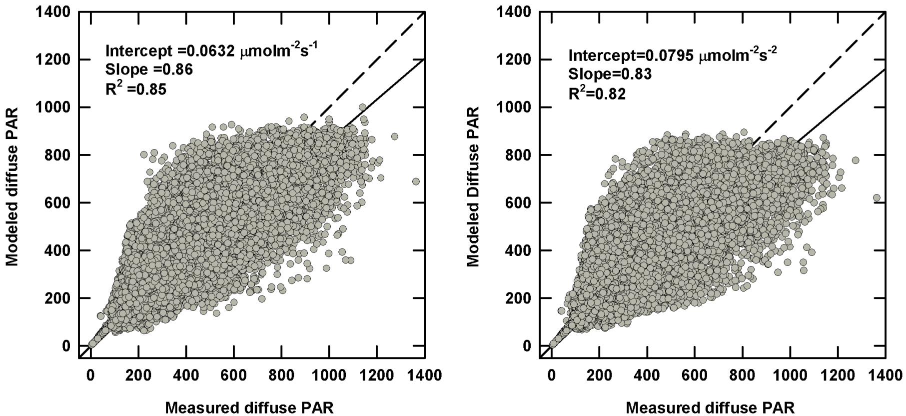

Fig. 4. Comparison between measured and modeled diffused PAR **(a)** logistic model **(b)** cubic polynomial model. The regression statistics presented are for the bootstrap regression between the measure and modeled variables. All units are in $\mu mol\,m^{-2}\,s^{-1}$.

CC BY

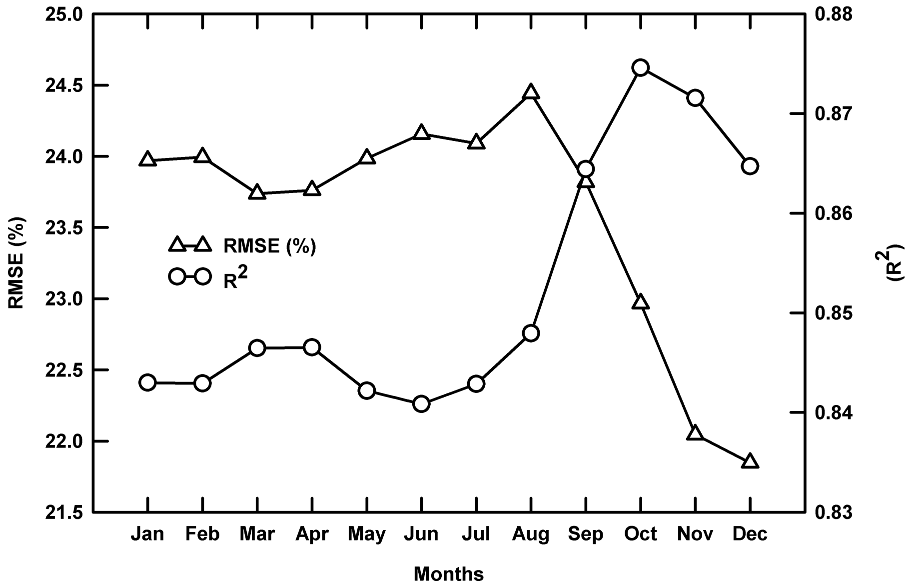

Fig. 5. Model performance in terms of RMSE (%) and R^2 over various months of the year.

GMDD
7, 1649–1669, 2014

Development of a semi-parametric PAR partitioning model

J. C. Kathilankal et al.

cc BY